European Polymer Journal 142 (2021) 110158

Contents lists available at ScienceDirect

European Polymer Journal

journal homepage: www.elsevier.com/locate/europolj

Coaxial and emulsion electrospinning of extracted hyaluronic acid and keratin based nanofibers for wound healing applications

Sena Su [a,b], Tuba Bedir [a,b], Cevriye Kalkandelen [a,c,*], Ahmet Ozan Başar [d,e], Hilal Turkoğlu Şaşmazel [f], Cem Bulent Ustundag [a,b], Mustafa Sengor [a,g,*], Oguzhan Gunduz [a,g]

[a] Center for Nanotechnology and Biomaterials Application and Research (NBUAM), Marmara University, 34722 Istanbul, Turkey
[b] Department of Bioengineering, Faculty of Chemical and Metallurgical Engineering, Yildiz Technical University, 34210 Istanbul, Turkey
[c] Biomedical Devices Technology, Vocational School Technical Science, Istanbul University-Cerrahpasa, 34500 Istanbul, Turkey
[d] Novel Materials and Nanotechnology Group, IATA-CSIC, 46980 Valencia, Spain
[e] R&D Department, Bioinicia S.L., 46980 Valencia, Spain
[f] Metallurgical and Materials Engineering Department, Faculty of Engineering, Atilim University, Incek, 06830 Ankara, Turkey
[g] Department of Metallurgical and Materials Engineering, Faculty of Technology, Marmara University, 34722 Istanbul, Turkey

ARTICLE INFO

Keywords:
Hyaluronic acid
Keratin
Emulsion electrospinning
Coaxial electrospinning
Wound healing

ABSTRACT

Novel composites based on poly(ε-caprolactone)/polyethylene oxide loaded with hyaluronic acid(HA) and keratin(KR) were produced separately using emulsion and coaxial electrospinning methods. HA and KR were extracted from animal sources, characterized and loaded into coaxial fiber structures as *bioactive agents*, separately and together. Morphological, chemical, thermal, and mechanical characteristics of the fibers were investigated. According to the SEM results, diameters of smooth and beadless fibers fabricated via emulsion method were at nanoscale (sub-micron) while fibers of coaxial method were at micro scale. Benefitted electrospinning techniques demonstrated that hydrophobic and hydrophilic polymers can be advantageously combined. Core polymer specific FT-IR bands were not visible, their presence was proven with DSC analysis which confirms core–shell morphology of the fibers. In vitro studies exhibited spun mats did not have any cytotoxic effects and the HA and KR incorporated into the fiber structure synergistically increased cell viability and cell proliferation. This study demonstrated that the electrospun fibers containing HA and KR fabricated by both emulsion and coaxial methods can be efficient for wound healing applications.

1. Introduction

Wound healing is a complicated process of tissue regeneration in which the body responds to the lost cellular structures as a result of different traumatic injuries [1]. To speed up this process, dressings like gels and creams are mostly applied clinically to the wound area [1,2]. However, clinical treatment can be a painful and costly process, especially for patients with diabetes-related ulcers [3]. Therefore, there is a need to develop innovative dressings containing bioactive components that will relieve recurrent painful procedures and increase the wound healing process.

Various methods like phase separation, template synthesis, melt blowing, self-assembly, and electrospinning have been used to produce polymeric fibers [1]. Among these methods, electrospinning draws more attention for wound healing applications as it is a simple, cost-effective and versatile method for producing drug-loaded fibers in nanometer-sized [4,5]. The porous surface of nanofibers produced by this method can mimic the extracellular matrix (ECM) that fills the gaps between the cells and connects and supports them [6,7]. Besides, these nanofibers can provide a high surface area, which creates a favorable environment for cell -attachment, growth, and proliferation [8,9]. In addition, the nanofiber dressing prevents the passage of any substance that can cause bacterial or microbial infection and allows the transition of oxygen required for wound healing thanks to its porous structure [8,10].

The electrospinning method allows the use of various natural and synthetic polymers to fabricate nanofibers. Among the synthetic polymers, poly(ε-caprolactone) (PCL) is a suitable candidate for wound dressing applications due to its biocompatibility, biodegradability, structural stability, and mechanical properties [11,12]. However, it is highly hydrophobic, and its degradation rate can be adjusted by mixing

* Corresponding authors at: Center for Nanotechnology and Biomaterials Application and Research (NBUAM), Marmara University, 34722 Istanbul, Turkey.
E-mail addresses: kalkan@istanbul.edu.tr (C. Kalkandelen), mustafa.sengor@boun.edu.tr (M. Sengor).

https://doi.org/10.1016/j.eurpolymj.2020.110158
Received 1 May 2020; Received in revised form 10 November 2020; Accepted 11 November 2020
Available online 21 November 2020
0014-3057/© 2020 Published by Elsevier Ltd.

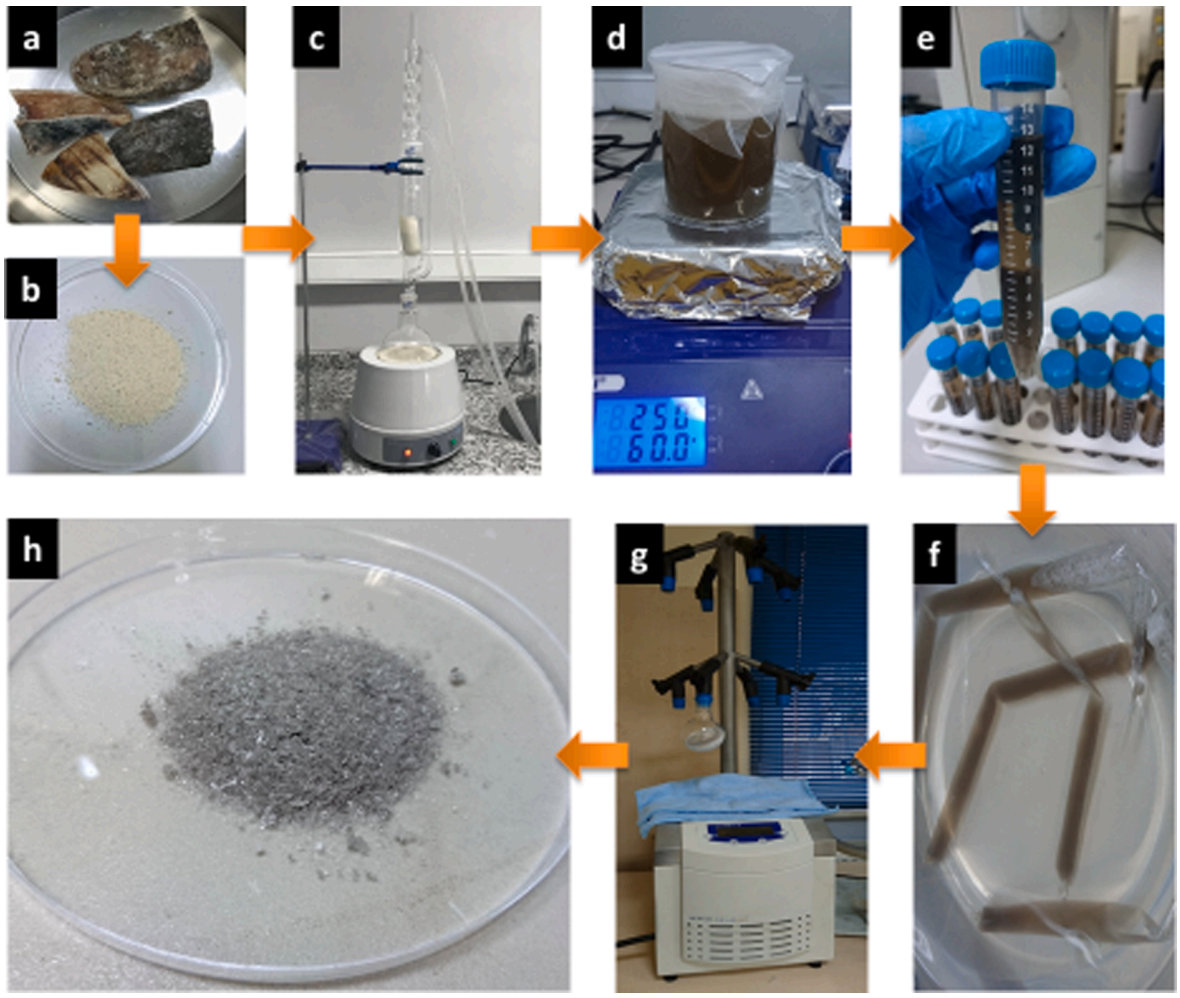

Fig. 1. KR extraction process (a) animal hooves, (b) powder hooves, (c) Soxhlet system, (d) chemical reduction process, (e) centrifuged tubes, (f) dialysis process, (g) lyophilization, and (h) powder keratin.

it with a hydrophilic polymer [13,14]. Polyethylene oxide (PEO) is a hydrophilic, non-toxic, biocompatible, and biodegradable polymer [15,16]. It rapidly degrades by interacting body fluid, therefore preferred as a drug carrier for wound dressing applications [15,17]. It has been shown that PEO blending to PCL highly develops the surface features owing to the hydrophilic structure of PEO [13].

Natural polymers are incorporated into the structure of nanofibers made of synthetic polymers in wound dressing applications to enhance compatibility with tissue and promote cell growth and proliferation [18,19]. Besides, natural polymers, which accelerate the wound healing process due to their structural similarities with ECM, have been shown to repair damaged tissues [20]. It cannot be electrospun alone owing to their molecular structure, therefore generally used together with synthetic polymers for nanofiber production [1].

Hyaluronic acid (HA) is a polysaccharide of the glycosaminoglycan group, which is naturally found in the ECM structure in tissue [21]. It exists in cockscomb, in synovial fluid, in the vitreous humour of the human eye, in the umbilical cord at high amounts [22,23]. Ensuring the moisture balance of the region in wound healing facilitates cell proliferation and migration [24]. Since HA is a hygroscopic macromolecule, it provides control of hydration in the region during wound healing [25]. Keratin is known to be one of the most abundant proteins in nature and is preferred in tissue engineering research due to its biocompatibility, biodegradability, and biofunctionality [26,27]. It is found in hair, feathers, wool, nails, horns, and hooves in mammals [28,29]. The use of keratin in tissue-engineered scaffolds has been shown to promote cell adhesion and proliferation also enhance tissue biocompatibility of the material, both in vitro [29] and in vivo [30,31].

Different methods have been developed for the incorporation of bioactive molecules into nanofibers by electrospinning such as blend, coaxial, and emulsion electrospinning. It has been indicated in previous studies that coaxial and emulsion electrospinning techniques show superior properties in preserving the properties of bioactive molecules used and drug release studies compared to the blend electrospinning [4,32]. By using emulsion and coaxial techniques, core–shell structured fibers can be produced in which the drug / bioactive agent can be effectively loaded [33]. It has been a matter of discussion by the researchers which technique is superior because both techniques have their advantages and disadvantages. Emulsion electrospinning compared to coaxial, is a more common technique in terms of providing protein dissolution in a soft solvent, and it has a simpler setup [34,35]. However, maintaining precise control over the placement of the drug in the core or shell of the structure is one of the advantages of using coaxial electrospinning instead of emulsion [33,36].

In this study, nanofiber wound dressings containing bioactive substances that accelerate wound healing were produced for wounds such as burns and diabetes-related ulcers. Hyaluronic acid and keratin as bioactive substances were extracted from animal sources and characterization studies were performed. The obtained keratin and hyaluronic acid were incorporated into the core structure of poly(ε-caprolactone) and polyethylene oxide polymers and the fibers were produced by emulsion and coaxial electrospinning techniques. The morphology,

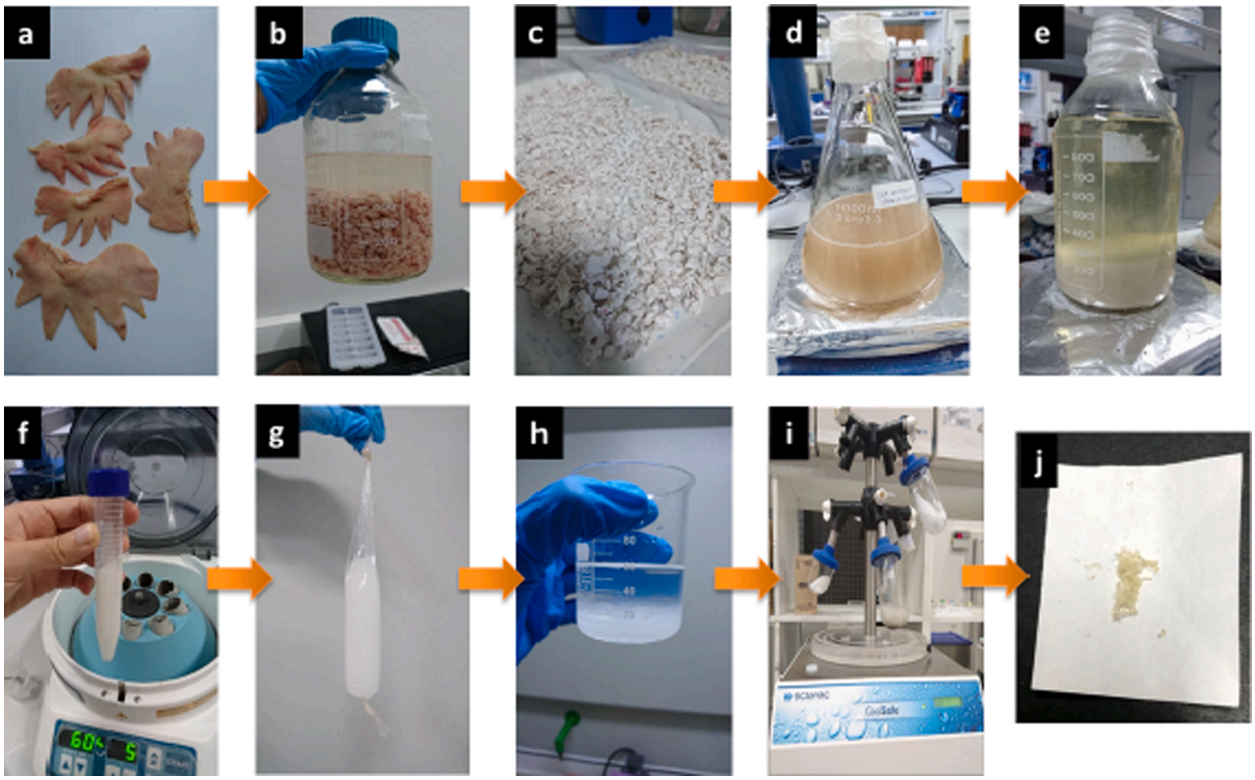

Fig. 2. HA extraction process (a) rooster combs, (b) treatment with acetone, (c) dried combs, d) extract, (e) precipitation of the extract with ethanol, (f) centrifugation process, (g) dialysis process, (h) final precipitate, (i) lyophilization, and (j) powder HA.

chemical bond structure, thermal behavior, and mechanical strength of the fibers produced by adding hyaluronic acid and keratin separately and together were investigated. The effects of bioactive substances and two different methods on fiber structures were investigated by detailed characterization tests.

2. Materials and methods

2.1. Materials

Hexane, Urea, Sodium Dodecyl Sulfate (SDS), 2-Mercaptoethanol, Acetone, Sodium Acetate, Ethanol, Chloroform, and Amyl alcohol were purchased from Merck KGaA, Germany. Dichloromethane (DCM, ≥99.0% pure) was bought from ISOLAB, Germany. Poly(ϵ-caprolactone) (PCL, the weight-average molecular weight of 80,000 g/mol) and Tween-80 (surfactant) were purchased from Sigma-Aldrich, UK. Polyethylene oxide (PEO, the weight-average molecular weight of 600 g/mol) and dialysis membrane (cut-off value 14 kDa and average flat width 43 mm) were obtained from Sigma-Aldrich, USA. For cell cultivation, Dulbecco's Modified Eagle Medium (DMEM/F12), PBS (phosphate buffer saline), 3-(4,5- dimethyl-2-thiazol)-2,5-diphenyl-2H-tetrazolium bromide (MTT) powder, penicillin/streptomycin, L-glutamine, fetal bovine serum (FBS), Trypsin/EDTA solution, trypan blue, dimethylsulfoxide (DMSO), ethanol with ≥ 99.8% (vol./vol.), glutaraldehyde, acridine orange base (AO), propidium iodide (PI), and hexamethyldisilazane (HMDS) with ≥ 99% were purchased from Sigma Aldrich Co. (St. Louis, USA).

2.2. KR an HA extraction from animal tissues

Keratin (KR) was obtained from animal hooves by using the procedure reported by Kakkar et al. [37]. Cattle hooves from the slaughterhouse (Fig. 1a) were divided into small pieces mechanically and then passed through the grinder to be powdered, as shown in Fig. 1b. Powdered hooves were passed through the soxhlet system (Fig. 1c) to degrease for 3 days. Hexane: dichloromethane (1:1) was used as a solvent. Degreased cattle hooves were thrown into a mixture of 7 M urea, 6 g SDS and 15 ml 2-mercaptoethanol and reduced with stirring at 60 °C for 12 h (Fig. 1d). Then, centrifuged at 60 rpm for 15 min, the filtrates were taken (Fig. 1e) and dialyzed against distilled water in the dialysis membrane for 5 days (Fig. 1f). The dialyzed keratin solution was dried at −70 °C in a freeze dryer (Fig. 1g). The powder keratin was obtained as the final product (Fig. 1h).

Hyaluronic acid (HA) was extracted from rooster combs according to the literature presented by Kang et al. with minor modifications [38]. Combs of slaughtered roosters were obtained from Erpilic Integrated Poultry Production and Trade Ltd. and frozen at −20 °C (Fig. 2a). 500 g of frozen rooster combs were crushed to a size of 0.5 cm. They were treated with acetone for degreasing in a soxhlet device for 2 days (Fig. 2b). The degreased rooster combs were dried (Fig. 2c). The rooster combs were kept in 1 L 5% sodium acetate solution, and extracted by squeezing with a cotton swab every 2 h (Fig. 2d) and the remaining residue was discarded. 1.5 L ethanol was added to the liquid extract for precipitation and the precipitate was centrifuged (Fig. 2e). The filtrate was discarded, and the residue was re-centrifuged by dissolving in 5% sodium acetate solution (Fig. 2f). After rinsing with 100 ml of chloroform, the chloroform: amyl alcohol (1:2) was mixed with the solvent mixture until the gel formation disappeared. The final solution was taken to the dialysis membrane (cut-off value 14 kDa) and dialyzed against distilled water for 3 days (Fig. 2g). The dialysis solution was precipitated with ethanol, and the precipitate (Fig. 2h) was lyophilized (Fig. 2i). The obtained powder HA is shown in Fig. 2j.

2.3. KR and HA characterization tests

The chemical structures of the KR and HA were analyzed by Fourier Transform Infrared Spectrophotometer (FTIR, Jasco, FT/IR-ATR 4700) equipped with an ATR-crystal prism accessory. Attenuated total

reflection (ATR) is an apparatus that allows to determine chemical composition of the surface of solid samples without sample preparation like compression samples with Potassium Bromide (KBr) until forming a disk [39,40]. The spectra were collected at wavelengths in the range of 4000 cm^{-1} to 450 cm^{-1} with 32 running scans at a resolution of 4 cm^{-1}.

SDS-PAGE (Polyacrylamide Gel Electrophoresis), is a versatile and high-resolution method used to separate components of a protein mixture based on their size [41]. The separation of proteins by electrophoresis is based on charged molecules migrates through a matrix upon application of an electrical field [42].

The molecular weight distribution of keratin was measured by sodium dodecyl sulphate–polyacrylamide gel electrophoresis (SDS-PAGE) method according to Laemmli [43] by using 5% (w/v) stacking gel and a 10% (w/v) resolving gel a Mini Protean II unit (Bio-Rad Laboratories, Hercules, CA, USA). Before the SDS PAGE, the protein concentration in the KR extract was estimated by using the Pierce bicinchoninic acid (BCA) protein assay kit (Thermo Fisher Scientific, USA). The liquid keratin was mixed with a sample buffer containing SDS and β-mercaptoethanol to achieve a final protein concentration of 2 mg/ml. The samples were denatured by heating at 80 oC before they were loaded onto the gel. Electrophoresis was performed at a constant 120 V for 15 min and 100 V for 80 min in the Tris-base buffer, pH 8.5. After the electrophoresis protein bands were stained with Coomassie brilliant blue R- 250. Precision Plus protein standards all blue (Biorad) containing ten proteins within 250–10 kDa range was used as a molecular weight marker and the gel was visualized with the Image Analyzer System (Chemi Doc MP Imaging System-BioRad, USA).

Analysis of produced HA was carried out with gel permeation chromatography (GPC) at 30 °C at a flow-rate of 0.5 ml/min on a system consisting of an EcoSEC GPC System (HLC-8320) (Tosoh Bioscience) equipped with RI and UV detectors. The sample was first dissolved in PBS (pH: 7.4) at a concentration of 3 mg /ml and passed through a Sartorius RC 0.45 μm filter before the analysis.

^{1}H NMR spectra of HA were obtained using a Varian Unit Inova 500 nuclear magnetic spectrometer (Varian Unit Inova 500, USA) operated at 500 MHz, spectrometer operating at a temperature of 25 °C. All samples were dissolved in a mixture H_2O/D_2O, 90/10 v/v with a total volume equal to 600 μl.

2.4. Electrospinning process

Core-shell structured fibers are produced by both coaxial and emulsion electrospinning techniques, as represented in graphical abstract. In coaxial electrospinning, two different solutions are connected to the electrospinning system using a coaxial needle. In the emulsion electrospinning, a hydrophilic polymer solution (water phase) is slowly added into the hydrophobic polymer solution (oil phase) and homogenized with a homogenizer to form an emulsion polymer solution. The emulsion solution is connected to the electrospinning system with a single needle.

2.4.1. Production of fibers by emulsion electrospinning

PCL solution (oil phase) was prepared at a concentration of 8% (w/v) in chloroform: dimethylformamide (12:1 v/v) and PEO solution (water phase) was prepared at a concentration of 4% (w/v) in distilled water. Then, 1 wt% emulsifier (Tween-80) was added to the PCL solution, the PEO solution was added dropwise into the PCL solution and stirred on a magnetic stirrer. A homogeneous emulsion solution was obtained by a homogenizer. The emulsion solution was taken into a 5 cc syringe, and an electrospinning process was started. The electrospinning parameters (voltage, flow rate, the distance between needle tip-collector) were optimized to obtain uniform nanofiber morphology. After optimization, 2 wt% KR and 2 wt% HA were added separately and together (1 wt% KR:1wt%HA) to the PEO solution for inclusion in nanofiber structure. The nanofibers were prepared using an electrospinning device (NS24, Inovenso Co., Istanbul, Turkey). The distance between the tip of the needle and the grounded collector was adjusted as 19 cm and a voltage of 21 kV was applied by a high-voltage power supplier for electrospinning. The flow rate of the emulsion solution was 0.8 ml/h. The used needle has a diameter of (OD: 1.30 mm, ID: 1.20 mm). All the experiments were carried out at ambient conditions.

Table 1
Components of the core–shell structured nanofibers produced by emulsion and coaxial electrospinning techniques.

	Sample Name	Shell	Core
Emulsion	E	8% PCL	4% PEO
	E-KR	8% PCL	4% PEO + 2% KR
	E-HA	8% PCL	4% PEO + 2% HA
	E-KR + HA	8% PCL	4% PEO + 1% KR + 1% HA
Coaxial	C	8% PCL	4% PEO
	C-KR	8% PCL	4% PEO + 2% KR
	C-HA	8% PCL	4% PEO + 2% HA
	C-KR + HA	8% PCL	4% PEO + 1% KR + 1% HA

2.4.2. Production of fibers by coaxial electrospinning

As in the previous method, PCL solution for the shell was prepared at a concentration of 8% (w/v) in chloroform: dimethylformamide (12:1 v/v) and PEO solution for the core was prepared at a concentration of 4% (w/v) in distilled water. Coaxial electrospinning was conducted by connecting the outer and inner needles to syringes containing shell solution and core solution. After optimizing the electrospinning parameters, KR 2 wt%, HA 2 wt%, and KR 1 wt% - HA 1 wt% were added to the PEO solution, respectively. The prepared three solutions were connected to the inner needle and the PCL solution was connected to the outer needle. The inner needle has a diameter of (OD: 1.30 mm, ID: 1.20 mm) and the outer needle has a diameter of (OD: 2.13 mm, ID: 1.88 mm). The electrospinning process was performed at 22.5 kV applied voltage and the distance between the collector cylinder and needle tip was 19 cm. The flow rates of a shell (PCL) and core (PEO + bioactive components) solutions were 0.8 ml/h and 0.6 ml/h, respectively. All the experiments were carried out at ambient conditions.

Abbreviations of the groups were listed as in Table 1.

2.5. Characterization of electrospun fibers

2.5.1. Scanning electron microscopy (SEM)

The morphologies of the electrospun fibers (E, E-KR, E-HA, E-KR + HA, C, C-KR, C-HA, C-KR + HA) produced by emulsion and coaxial electrospinning methods were observed by SEM (EVA MA 10, Zeiss, San Diego, CA, USA) at an accelerating voltage of 10 kV. Before observation, the fibers were sputter-coated with gold/palladium by a coating device (SC7620, Quorum, Lewes, UK). 100 fibers were randomly measured from each sample using imaging analysis software to determine average fiber diameter and diameter distribution (SmartSEM, Zeiss, San Diego, CA, USA).

2.5.2. Fourier-Transform infrared spectroscopy (FT/IR)

Same, ATR-FTIR device for the characterization of the raw materials was used to observe the spectral absorption peaks of fiber samples. Fibers turned into small clusters to take data.

2.5.3. Differential scanning Calorimetry (DSC)

The thermal characterization of the fiber samples was performed using a differential scanning calorimeter (DSC-60 Plus, Shimadzu, Japan). All the samples (~3 mg for each) were placed into aluminum pans and heated from 20 to 200 °C under nitrogen gas at a rate of 10 °C/min.

2.5.4. Water contact angle

Water contact angle was measured by the sessile drop method (drop

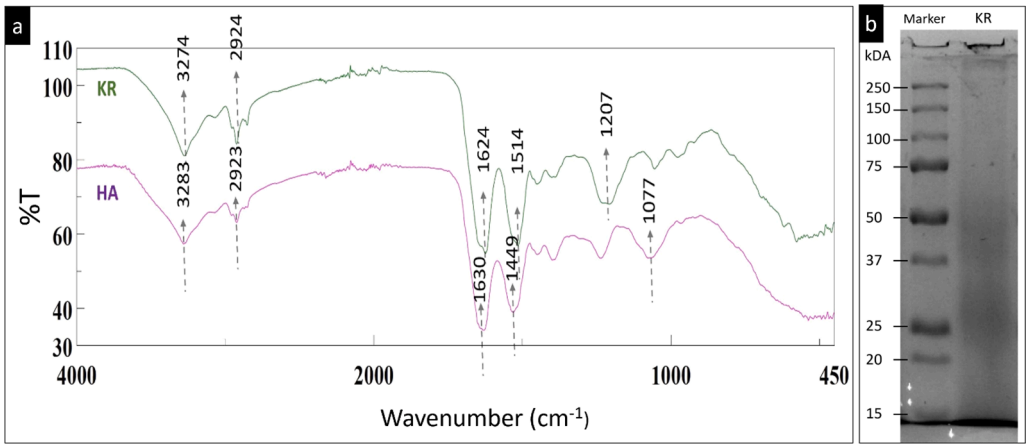

Fig. 3. (a) FT-IR spectrums of KR and HA and (b) SDS-PAGE result of KR extract.

shape analysis system DSA-100/10, Kruüss) at room temperature. DI water (3 µl) was dropped onto each sample and its evolution in 3 s was recorded with a CCD camera and at least three measurements were taken from different places.

2.5.5. Mechanical testing

Tensile tests were performed to determine the mechanical properties of the fiber samples. The tests were conducted on the Shimadzu (Japan) EZ-LX model tensile test device equipped with a load cell of 5 kN ± 0.5% and having a displacement resolution of 1 µm at room temperature (23 °C). Three specimens of each sample were cut (1x5 cm), and their thickness was measured with a digital micrometer (293–100, Mitutoyo, Japan). The speed of the tensile test was 5 mm/min.

2.5.6. Cell culture studies

2.5.6.1. Cell attachment. Cell proliferation on the fabricated mats was examined with L929 ATCC CCL-1 mouse fibroblast cells. Electrospun mats of 1.5 cm diameter were placed in 24 well-plate Petri dishes and followed by the exposure to ultraviolet (UV) radiation for 10 min for sterilization purposes. Cell viability studies were performed for 7 days with the initial cell seeding concentration of 5×10^4 cell/ml in a culture medium that consisted of: DMEM/F12 + 10% in volume (vol.-%) of FBS + 1 vol-% penicillin + streptomycin (100 units/ml penicillin, 100 µg/ml streptomycin) + 1 vol-% L-glutamine. The cultured electrospun samples in Petri dishes were then kept in an incubator at 5% CO_2 and 37 ℃ and the medium was replaced every other day for 7 d. For all of the culture studies, a standard tissue culture polystyrene (TPCS) plates were used as control.

The degree of cell attachment was examined by the haemocytometer counting method for 3 h at the following time intervals: 30, 60, 90, 120, 150, and 180 min. For this, the medium from each well was discarded to remove unattached cells. Then, the samples were incubated for 15 min at 37 ℃ in Trypsin/EDTA solution (0.1% wt./vol.) to harvest attached cells after the incubation. Thereafter, the remaining cells were counted for each time internals by the trypan blue dye exclusion technique. The attachment results were expressed as the percentage of viable cells in relation to the initially seeded cells.

2.5.6.2. MTT assay. The 3-(4,5-dimethylthiazol-2-yl)-2,5- diphenyltetrazolium bromide) (MTT) assay was carried out at the end of 3rd, 5th, and 7th days. After the incubation, the medium of the electrospun mats was discarded and the mats were washed with PBS 3 times. Then, 600 µl of fresh medium and 60 µl of MTT solution were added to be followed by the incubation for 3 h. After, the medium was removed and replaced with 1 ml of dimethylsulfoxide (DMSO) in order to dissolve formazan crystals and then, the samples were placed into the incubator for another hour. Finally, for the measurement, 200 µl were taken from each solution and placed into 96-well plates. Cell viability, in terms of absorbance, was determined by Dynamica LEDETECT96 microplate reader (Livingston, UK) at 540 nm. Each measurement was done in triplicate.

2.5.6.3. Fluorescence microscopy analyses. Fluorescence images were taken on the 3rd and 7th days of the culture using a fluorescence microscope AMG EVOS-FL from Thermo Fisher Scientific (Mill Creek, USA). For staining, AO (25 µg/ml) and PI (25 µl/ml) dye solutions were used. Initially, the samples were taken out from the incubator and each well plate medium was removed and washed with PBS three times. The fixation was carried out with 2.5 vol-% glutaraldehyde for 30 min and stained with an AO/PI (vol./vol.) solution in the dark for 10 min at room temperature.

2.5.6.4. SEM characterization. SEM images were taken on the 7th day of cell cultivation. For this, each well medium was discarded and the samples were washed with PBS three times. The mats were fixed with 2.5 vol-% glutaraldehyde for 30 min at room temperature. Thereafter, the mats were dehydrated with different concentrations of ethanol, i.e. 30, 50, 70, 90, and 100 wt-%, for 2 min each, and then immersed in pure HMDS for 5 min and air-dried.

2.5.6.5. Statistical analysis. All experiments were repeated three times (n = 3). The statistical differences were determined with one-way analysis of variance (ANOVA) followed by Tuckey's test using IBM SPSS v24.0 Statistics software. Probability of the data was considered statistically significant for p values$<$0.05 and statistically highly significant for p values$<$0.01. The results were marked with (*) for $p < 0.05$.

3. Results and discussion

As shown in Fig. 3a, the FT-IR spectrum of KR displayed characteristic peaks at 3274 cm^{-1} (amide A), 2924 cm^{-1} (amide B) 1624 cm^{-1} (amide I) ve 1514 cm^{-1} (amide II), 1207 cm^{-1} (amide III) bands. These results agree with the findings of the previous studies [30,37,44]. HA spectrum showed —OH stretching vibrations at 3283 cm^{-1} and CH2 stretching vibrations at 2923 cm^{-1}. The peaks at 1630 cm^{-1}, 1449 cm^{-1}, and 1077 cm^{-1} were attributed to the presence of amid II, C-0 group with C = O combination and C-0-C stretching, respectively. These results were consistent with those of other studies [45,46].

The protein concentration in the KR extract was found 0,02 mg/ ml as a result of the BCA protein assay kit. SDS-PAGE analysis which frequently used in characterization of protein structure, was performed to confirm produced KR structure and estimate its molecular weight. The

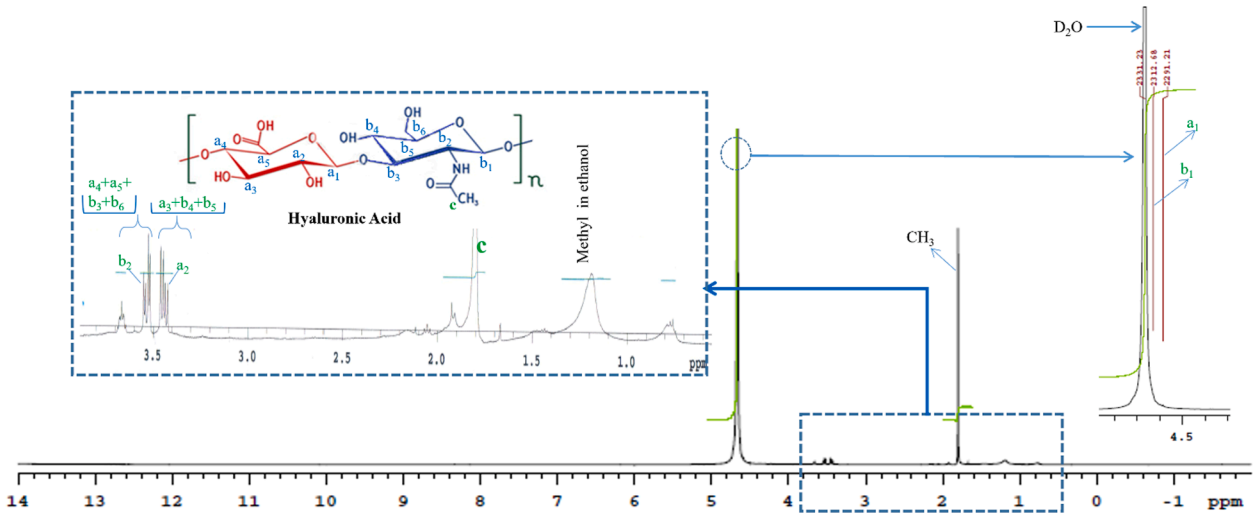

Fig. 4. NMR spectrum of HA.

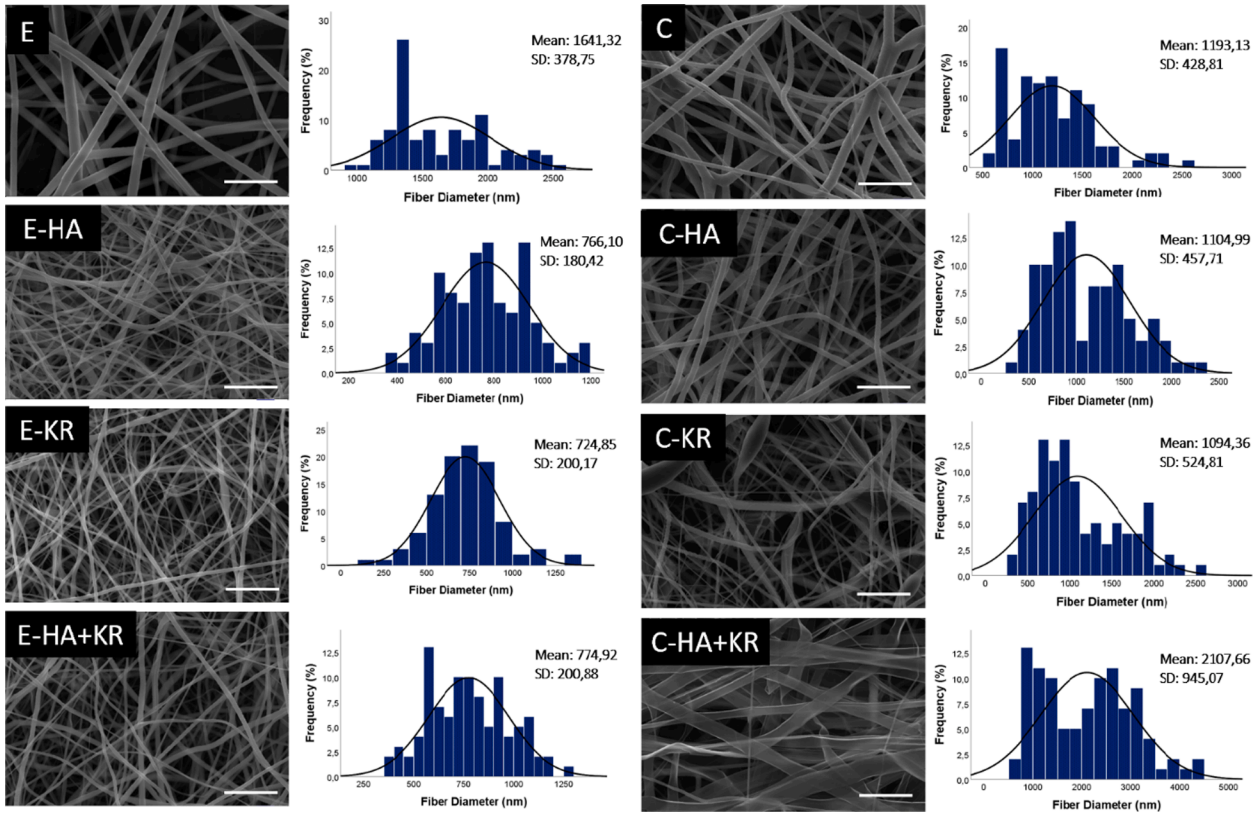

Fig. 5. SEM images and mean fiber diameter distributions of the fiber samples produced by emulsion and coaxial electrospinning techniques. The scale bar represents 10 μm.

molecular weight distribution of the KR extract exhibited a clear protein fraction between 40 and 60 kDa associated with type II (basic) keratin, as shown in Fig. 3b. The bands are observed between 23 and 30 kDa were related to keratin-associated proteins (KAPs) [47]. These results were consistent with previous studies about the extraction of the keratin from hard tissues [37,48].

According to the GPC results, the profile observed for HA shows a homogeneous distribution with an average molar mass of 1.78×10^6 g mol^{-1}, which proves that hyaluronic acid with higher molar weight was produced.

Fig. 4 showed the NMR analysis results of HA obtained from rooster combs and the peaks indicated at 1.79 ppm are attributed to the methyl group in HA [49–51] while the weak peak at 1.15 ppm is attributed to the methyl group in ethanol [52]. In addition, the peaks in the range of (3.42–3.55) ppm were attributed to the sugar chains in HA and assigned according to their corresponding protons as shown in Fig. 4 [53]. 4.6 ppm and 4.8 ppm are the dH_2O peaks. Thus, ^1H NMR results proved that HA was successfully produced.

SEM images and average fiber diameter distributions of E, E-KR, E-HA, E-KR + HA, C, C-KR, C-HA, C-KR + HA samples were shown in Fig. 5. In general, it can be observed that the fibers produced by emulsion electrospinning are at the nanoscale (sub-micron), and the fibers

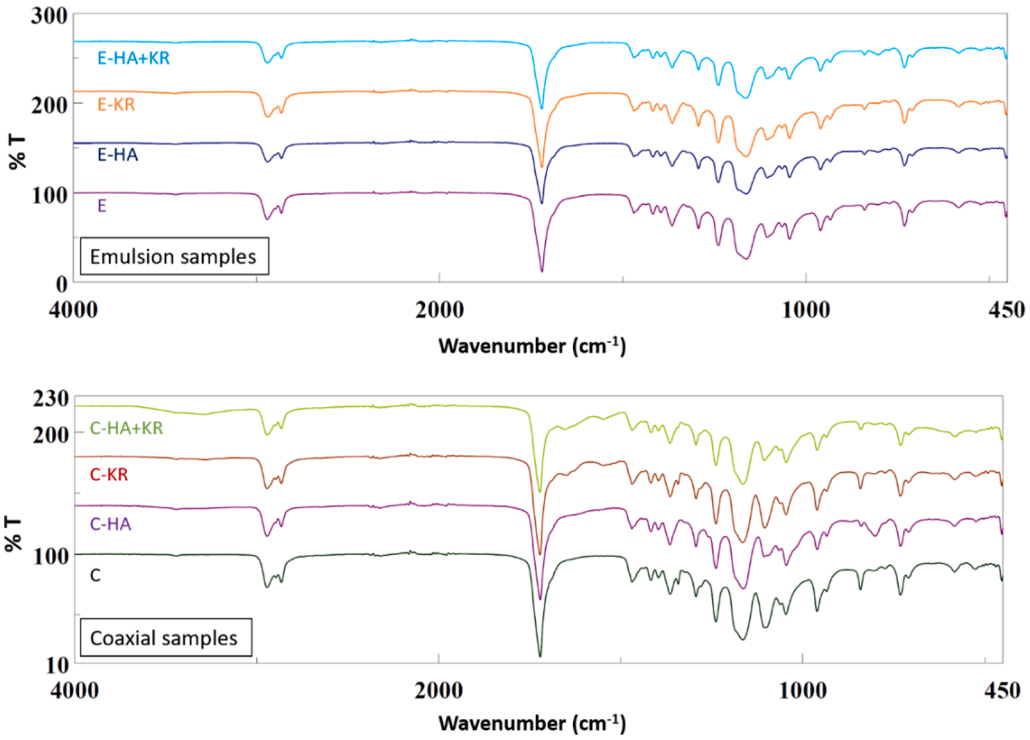

Fig. 6. FTIR-ATR spectrum of core–shell structured fibers produced by coaxial and emulsion electrospinning techniques.

produced by coaxial electrospinning are at the micro-scale. Considering that there were double flows from syringes in the coaxial technique, this is an expected result. Besides, it can be seen that all emulsion nanofiber samples showed smooth and beadless fiber morphology and nanofibers became thinner by the addition of KR and HA. This result may be explained by the fact that the conductivity of the spinning solution with presence of HA and KR due to their polyanionic and polar properties [54,55]. It is well known that the higher conductivity of solutions leads to thinner nanofibers in the electrospinning technique.

It has been also shown in the literature that the use of KR and HA has an effect on the reduction of the diameters of nanofibers [56–58]. For fibers produced by coaxial technique, C and C-HA samples also showed bead-free and smooth fiber morphology. However, the fiber structure exhibited the tendency for bead formation in the presence of KR. Although HA and KR were used separately (C-HA and C-KR samples), there was no significant change in diameter compared to the C sample. As shown in Fig. 5; C-HA + KR fibers differ from the classical cylindrical structure and exhibit a ribbon-flat structure. This has been reported in the literature to be related to the rapid evaporation of the solvent during the electrospinning of high-density electrospinning solutions [59,60].

FTIR spectra of E, E-KR, E-HA, E-KR + HA, C, C-KR, C-HA, C-KR + HA samples were given in Fig. 6. The spectra of both groups show characteristic infrared bands of PCL. The peaks indicated at 2941 cm^{-1}, and 2864 cm^{-1} were due to asymmetric —CH2 stretching and symmetric —CH2 stretching, respectively. Moreover, 1720 cm^{-1} band is assigned to the C═O group and 1293 cm^{-1}, and 1238 cm^{-1} bands were associated with C-O/C-C stretching and C-O-C asymmetric stretching, respectively [61]. According to the working principle of the FTIR-ATR technique, only the surface composition of the coaxial fibers can be examined. Therefore, the characteristic peaks of polymers such as PEO, HA and KR remaining in the inner layer were not expected to be seen in the FT-IR spectrum of coaxial nanofibers. The absence of peaks of the polymers remaining in the inner layer of the nanofibers produced by both techniques was the evidence of the core–shell structure. Similar findings have been shown in a previous study on coaxial nanofibers [62].

Differential Scanning Calorimetry thermograms of the core–shell fibers produced by two different methods were revealed in Fig. 7 and their melting temperatures and enthalpy values were presented in Table 2. Sample E recorded as the highest melt temperature (Tm) and the highest enthalpy of melting (ΔHm) at 61.60 °C and 27.74 J/g, respectively. E-KR + HA and C-KR + HA samples had the lowest melting temperature among other samples, as seen in Table 2.

The decrease in enthalpy and melting temperature with the addition of KR and HA can be related to the weak intra van der Waals bonds between PEO polymer molecules as shown in previous studies that dealt with only water-soluble polymers [56,63]. The crystallinity of PEO can be restrained due to formation of interpolymer complexes with hydrogen bonding between PCL and PEO which can be depicted from enthalpy info. Similar results also can be found for PEO/PAA in which PAA prohibited the formation of crystalline PEO [64]

Another interesting finding was that a second peak was observed in the C-HA + KR sample. This may be due to a kind of phase transition result associated with moisture loss. A similar finding was seen in a previous study [65]. The only difference from the coaxial and emulsion electropsining from material perspective is surfactant Tween-80. Tween 80 is known for its plasticizing effect [66]. Strain and tensile strength values can barely reflect this fact. The effect is expected to be low as it participates in very small amounts. Also crystallinity degree of PEO due to inter-polymer complexes with PCL could have effect the mechanical performances of the samples as Tween-80 stimulates the strength of the interfacial interactions. Fig. 7 shows the slight difference between Sample E and C. The same effect can be seen in the mechanical test results (Supplemantary S1). Modulus of the Sample C (tween80 free) is higher than modulus of Sample E and has much higher toughness.

Strength and flexibility are the main criteria for wound dressing applications. Because an ideal wound dressing is expected to be strong enough not to take damage from external impacts and to be flexible enough not to interfere with movement/damage the tissue on which it is located.

Values of the tensile strength (MPa) and strain at break (%) of nanofibers which are produced by emulsion and coaxial technique are

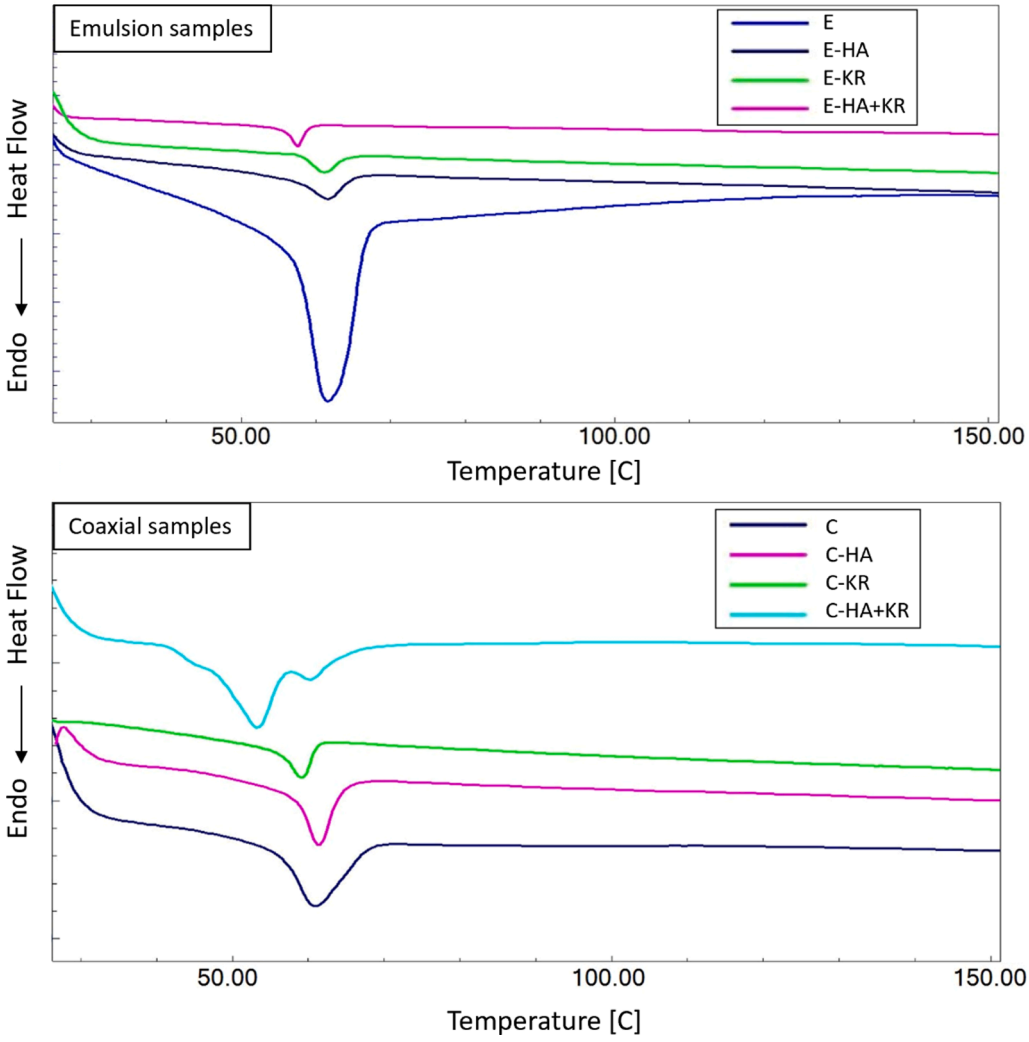

Fig. 7. DSC curves of fibers produced by coaxial and emulsion electrospinning techniques; E, E-HA, E-KR, E-HA + KR, C, C-HA, C-KR, and C-HA + KR.

Table 2
Melting temperatures and enthalpy values with tensile properties of electrospun fibers.

Sample name	DSC		Mechanical Tests		Sample name	DSC		Mechanical Tests	
	Tm (°C)	ΔHm (j/g)	Tensile Strength (MPa)	Strain at break (%)		Tm (°C)	ΔHm (j/g)	Tensile Strength (MPa)	Strain at break (%)
E	61.6	27.74	6.8 ± 0.2	319 ± 9.5	**C**	60.77	15.65	6.2 ± 0.3	171 ± 5.1
E-HA	61.66	6.15	5.9 ± 0.2	299 ± 11.9	**C-HA**	61.6	13.6	3.7 ± 0.1	37 ± 1.8
E-KR	61.17	6.08	14 ± 0.7	452 ± 18.0	**C-KR**	59.15	8.13	6.3 ± 0.2	155 ± 7.7
E-HA + KR	55.29	4.65	2.2 ± 0.1	158 ± 7.9	**C-HA + KR**	55.14	10.44	15.8 ± 0.6	118 ± 4.7

shown in Table 2. No significant change was observed between the maximum tensile strength of E and C samples (6.2 and 6.8 MPa). However, the E sample has an elongation of 299%, which was very flexible compared to C with an elongation of 171%. When HA was added to the structure, the maximum deformation decreased in the coaxial and emulsion samples to 3.7 MPa and 5.9 MPa, respectively. Thus, HA, which is known for its hydrophilic structure, has been shown to result in the weakening of the mechanical properties of nanofibers [67]. KR-containing samples showed better mechanical and elongation properties than HA addition. The strength and strain values of the E-KR samples were higher than that of the C-KR samples due to the fact that emulsion nanofibers had more uniform and thin structure. Strength properties of E-HA + KR nanofibers meshes decreased while the C-HA + KR increased. This can be associated with the ribbon-flat morphology of the coaxial sample mentioned before in the morphological analysis section. It has been seen in the literature that the strength of flat fibers is considerably increased and the number of elongation decreased compared to cylindrical fibers. The tensile strength and strain values of C-HA + KR fibers were consistent with a similar study [60]. Based on these results, it can be concluded that the produced core–shell fibers are the good candidates that can be used in wound dressing applications.

Cell culture studies were carried out by culturing L929 mouse fibroblast cells on the fabricated electrospun mats. Fig. 8 (i) shows the degree of cell attachment in terms of expression of the percentage of viable cells about the seeded cells. As can be seen from the figure, cells successfully attached to both standard tissue culture polystyrene (TCPS) plates used as control and the fabricated electrospun mats. Even though the 3-D structures of electrospun mats were well-reported to promote

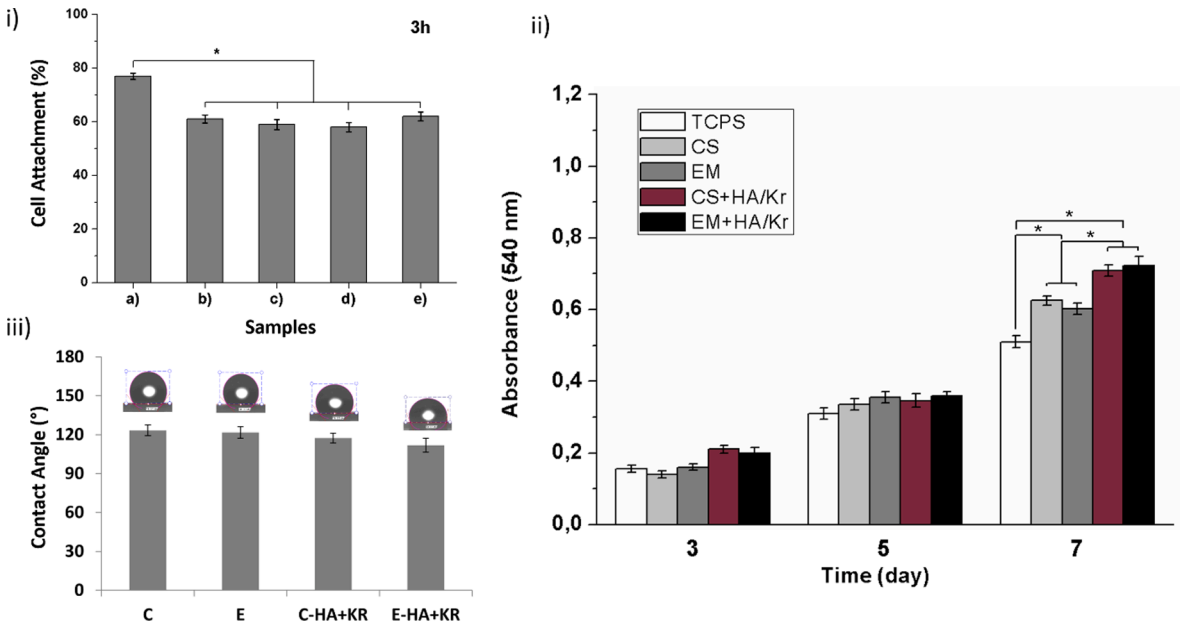

Fig. 8. (i)Percentage of cell attachment on the (a) TCPS plate as control and on the electrospun mats of: b) C; (c) E; (d) C- HA + KR; (e) E-HA + KR (*p < 0.05; data presented are mean ± SD, n = 3).(ii) Absorbance values of the electrospun mats obtained by MTT assay at 540-nm (*p < 0.05; data presented are mean ± SD, n = 3) (iii)Water contact angle values of the samples.

cell attachment performance [63], the control TCPS showed higher cellular adhesion, i.e. 77% vs ~ 60%. This result can be attributed to the wettability characteristics of the samples. It was previously reported in the literature that highly hydrophobic polymers, such as PCL, tend to exhibit relatively poor cell attachment performance [68]. In the case of electrospun emulsion and core–shell structures, hydrophobic polymer PCL, as the shell, might be responsible for the relatively poor cell adhesion results. Also, increasing the specific surface area by decreasing the fiber diameters is a well-known phenomenon which can be correlated to the cell attachment levels. As in Fig. 8(iii) C, E, E-HA + KR groups almost displayed the same wettability characteristics and C-HA + KR exhibited a lower cell attachment which is highly related to the mean fiber diameter size of 2107 mm. In addition to the effect of the chemical properties of the materials used in the structure, their morphology and surface roughness highly effect contact response of the interfaces.

The tetrazolium salt, MTT, an assay was performed to measure the cell proliferation rate. The viability of the cells is directly related to the level of reduction, which can be assessed with a spectrometer [68]. Fig. 8(ii) shows the cell viability of L929 fibroblasts on the fabricated electrospun mats for a seven-day period at time intervals of 48 h. As it can be seen from the figure, the electrospun mats exhibited no cytotoxicity as a consequence of the steady increase in absorbance values. At the 3rd and 5th days, no significant cell viability differences were observed for each group. By the seventh day, the electrospun mats showed a notable increase compared to the control group (TCPS) whereas the highest groups were the ones which were incorporated with HA and KR. This is due to the two facts; first, the 3-D structure of the electrospun mats can effectively promote cell proliferation by providing a higher surface to volume ratio, in particular during the late stage of cell culture [69]. Second, the bioactive substances incorporated within PEO (core) increased the cell viability synergistically. In the literature, it was previously reported that HA inhibits cell proliferation while promoting cell migration [69]. On the other hand, KR was found and reported widely to its cell viability enhancement features [28]. These two opposing phenomenons might be responsible for the relatively small absorbance increase in the groups having HA and KR compared to the other mats not having those bioactive agents. Additionally, according to the recent advancements in the literature, the core–shell nanofiber

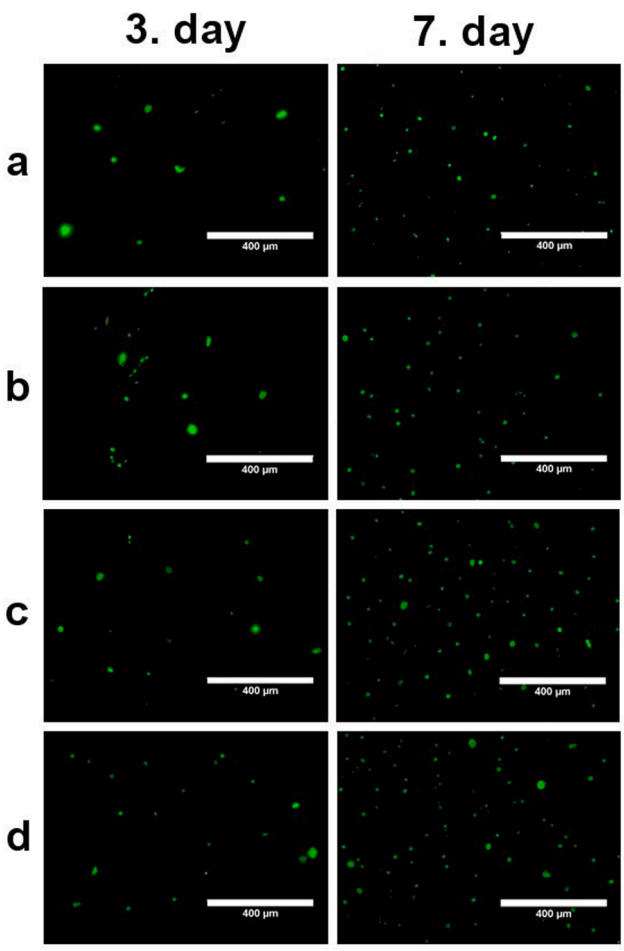

Fig. 9. Fluorescence images of the electrospun mats at 3rd day (left) and 7th day (right) of cell growth for: (a) C; (b) C-HA + KR; (c) E; (d) E- HA + KR. Scale markers of 400 µm in all cases.

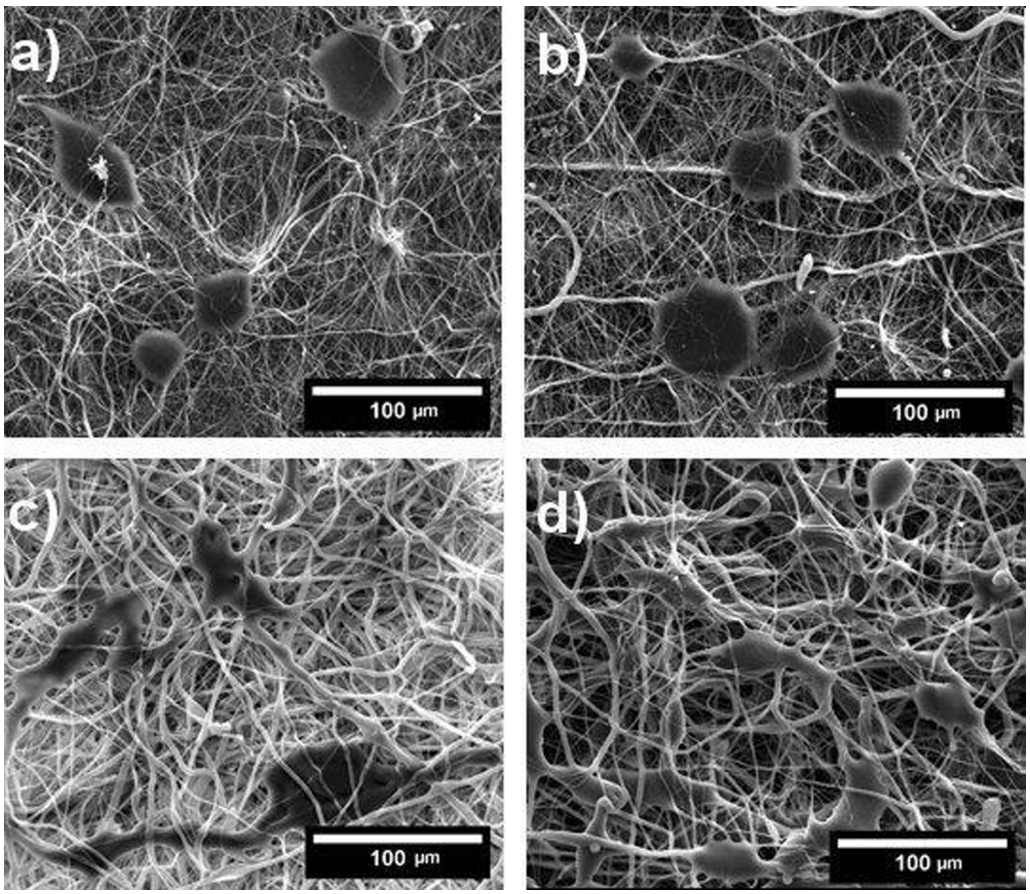

Fig. 10. SEM images of the cultured electrospun mats at 7th day of cell growth: (a) C-; (b) C-HA + KR; (c) E; (d) E-HA + KR. Scale markers of 100 µm in all cases.

structures can be achieved by coaxial or emulsion electrospinning [70]. This might be the reason that there were no significant absorbance value differences observed in terms of the core–shell and emulsion structures from the figure.

The fluorescence images (Fig. 9) for the previously dye stained electrospun mats exhibited similar results obtained in MTT assay. It can be seen from the figure that between the 3rd and 7th days the number of cells increased notably. On the 7th day, in terms of the cell density, no difference was observed for the core–shell and emulsion structures that had no bioagents (Fig. 9a,9b).

On the other hand, a slight increase of the cell density can be observed for the electrospun mats that contain HA and KR. Along with the MTT assay results, this suggests that the incorporation of HA and KR within polymer matrices promoted the cell proliferation synergistically. The cell morphology on the cultured electrospun mats was observed by utilizing SEM. On the 7th day of the culture cells exhibited notable proliferation on all fabricated mats (Fig. 10). It can be concluded from the figure that; all fabricated mats were biocompatible, which were in agreement with the MTT assay results of this study.

4. Conclusion

In this study, electrospun PCL / PEO fibers loaded with HA and KR natural polymers that increase biocompatibility and bioactivity were produced using emulsion and coaxial electrospinning methods. HA and KR were extracted successfully from the animal sources and FTIR, SDS PAGE and H-NMR analysis have revealed that HA and KR bioactive polymers were successfully obtained by chemical treatment from rooster combs and animal hooves, respectively. According to SEM results, it was observed that the emulsion method produced fibers on nanoscale, beadless, and smooth structure, while the coaxial method produced fibers on the micro-scale. Core-shell structured fibers showed a beadless and smooth fiber structure, however, beaded structure tendency was observed in samples with C-KR sample and C-HA + KR fibers showed a flat morphology. In FTIR-ATR analysis, only the characteristic bands of PCL, which is the shell polymer were observed. The fact that the bands of the core polymers are not seen in the results indicates that core–shell structured fibers were produced successfully. Tensile test results show that fiber samples have strength and elongation values in the appropriate range for wound dressing applications. Thermal characterization results demonstrate that fiber dressings can be used without any degradation or phase change at body temperature (35–38 °C). In vitro studies show that the electrospun mats did not exhibit cytotoxicity, and the bioactive substances incorporated into the fiber structure synergistically supported cell viability and cell proliferation. Moreover, these results are consistent with SEM observations. As a result of this study, electrospun fibers loaded with bioactive agents produced by both emulsion and coaxial methods were promising for wound dressing applications.

CRediT authorship contribution statement

Sena Su: Conceptualization, Methodology. **Tuba Bedir:** Conceptualization, Methodology. **Cevriye Kalkandelen:** Data curation, Writing - original draft. **Ahmet Ozan Başar:** Visualization, Investigation. **Hilal Turkoğlu Şaşmazel:** Visualization, Investigation. **Cem Bulent Ustundag:** Validation. **Mustafa Sengor:** Writing - review & editing. **Oguzhan Gunduz:** Supervision, Writing - review & editing.

Declaration of Competing Interest

The authors declare that they have no known competing financial

interests or personal relationships that could have appeared to influence the work reported in this paper.

Acknowledgements

This study was supported by the Turkish Scientific and Technical Research Council (TÜBİTAK) under Project Number: 218S270 and this work has also been supported by Marmara University Scientific Research Projects Coordination Unit under grant number FEN-B-121218-0614.

Appendix A. Supplementary material

Supplementary data to this article can be found online at https://doi.org/10.1016/j.eurpolymj.2020.110158.

References

[1] M. Gizaw, J. Thompson, A. Faglie, S.Y. Lee, P. Neuenschwander, S.F. Chou, Electrospun fibers as a dressing material for drug and biological agent delivery in wound healing applications, Bioengineering 5 (2018) 1–28, https://doi.org/10.3390/bioengineering5010009.

[2] G.P. Sidgwick, D. McGeorge, A. Bayat, A comprehensive evidence-based review on the role of topicals and dressings in the management of skin scarring, Arch. Dermatol. Res. 307 (6) (2015) 461–477, https://doi.org/10.1007/s00403-015-1572-0.

[3] R.G. Frykberg, T. Zgonis, D.G. Armstrong, V.R. Driver, Diabetic Foot Disorders, A Clinical Practice Guideline, J. Foot Ankle Surg. 45 (2006) 1–66, https://doi.org/10.1016/S1067-2516(07)60001-5.

[4] S.-F. Chou, D. Carson, K.A. Woodrow, Current strategies for sustaining drug release from electrospun nanofibers, J. Control. Release 220 (2015) 584–591, https://doi.org/10.1016/j.jconrel.2015.09.008.

[5] O. Catanzano, R. Docking, P. Schofield, J. Boateng, Advanced multi-targeted composite biomaterial dressing for pain and infection control in chronic leg ulcers, Carbohydr. Polym. 172 (2017) 40–48, https://doi.org/10.1016/j.carbpol.2017.05.040.

[6] W. Ji, Y. Sun, F. Yang, J.J.J.P. van den Beucken, M. Fan, Z. Chen, J.A. Jansen, Bioactive Electrospun Scaffolds Delivering Growth Factors and Genes for Tissue Engineering Applications, Pharm. Res. 28 (6) (2011) 1259–1272, https://doi.org/10.1007/s11095-010-0320-6.

[7] T.J. Sill, H.A. von Recum, Electrospinning: Applications in drug delivery and tissue engineering, Biomaterials 29 (13) (2008) 1989–2006, https://doi.org/10.1016/j.biomaterials.2008.01.011.

[8] M. Zamani, M.P. Prabhakaran, S. Ramakrishna, Advances in drug delivery via electrospun and electrosprayed nanomaterials, Int. J. Nanomed. 8 (2013) 2997–3017, https://doi.org/10.2147/IJN.S43575.

[9] M. Jannesari, J. Varshosaz, M. Morshed, M. Zamani, Composite poly(vinyl alcohol)/poly(vinyl acetate) electrospun nanofibrous mats as a novel wound dressing matrix for controlled release of drugs, Int. J. Nanomed. 6 (2011) 993–1003, https://doi.org/10.2147/IJN.S17595.

[10] L. Tian, M.P. Prabhakaran, X. Ding, D. Kai, S. Ramakrishna, Emulsion electrospun vascular endothelial growth factor encapsulated poly(l-lactic acid-co-ε-caprolactone) nanofibers for sustained release in cardiac tissue engineering, J. Mater. Sci. 47 (7) (2012) 3272–3281, https://doi.org/10.1007/s10853-011-6166-4.

[11] Y. Lu, J. Huang, G. Yu, R. Cardenas, S. Wei, E.K. Wujcik, Z. Guo, Coaxial electrospun fibers: applications in drug delivery and tissue engineering: Biomedical coaxial electrospun fibers, WIREs Nanomed. Nanobiotechnol. 8 (5) (2016) 654–677, https://doi.org/10.1002/wnan.1391.

[12] A.P.D. Elfick, Poly(ε-caprolactone) as a potential material for a temporary joint spacer, Biomaterials 23 (23) (2002) 4463–4467, https://doi.org/10.1016/S0142-9612(02)00163-1.

[13] M. Ponjavic, M.S. Nikolic, J. Nikodinovic-Runic, S. Jeremic, S. Stevanovic, J. Djonlagic, Degradation behaviour of PCL/PEO/PCL and PCL/PEO block copolymers under controlled hydrolytic, enzymatic and composting conditions, Polym. Test. 57 (2017) 67–77, https://doi.org/10.1016/j.polymertesting.2016.11.018.

[14] X. Wei, C. Gong, M. Gou, S. Fu, Biodegradable poly(ε-caprolactone)–poly(ethylene glycol) copolymers as drug delivery system, Int. J. Pharm. 381 (1) (2009) 1–18, https://doi.org/10.1016/j.ijpharm.2009.07.033.

[15] M. Pakravan, M.-C. Heuzey, A. Ajji, A fundamental study of chitosan/PEO electrospinning, Polymer 52 (21) (2011) 4813–4824, https://doi.org/10.1016/j.polymer.2011.08.034.

[16] N. Bhattarai, D. Edmondson, O. Veiseh, F.A. Matsen, M. Zhang, Electrospun chitosan-based nanofibers and their cellular compatibility, Biomaterials 26 (31) (2005) 6176–6184, https://doi.org/10.1016/j.biomaterials.2005.03.027.

[17] Y.e. Yang, T. Xia, W. Zhi, L.I. Wei, J. Weng, C. Zhang, X. Li, Promotion of skin regeneration in diabetic rats by electrospun core-sheath fibers loaded with basic fibroblast growth factor, Biomaterials 32 (18) (2011) 4243–4254, https://doi.org/10.1016/j.biomaterials.2011.02.042.

[18] G.D. Mogoşanu, A.M. Grumezescu, Natural and synthetic polymers for wounds and burns dressing, Int. J. Pharm. 463 (2) (2014) 127–136, https://doi.org/10.1016/j.ijpharm.2013.12.015.

[19] P. Zahedi, I. Rezaeian, S.-O. Ranaei-Siadat, S.-H. Jafari, P. Supaphol, A review on wound dressings with an emphasis on electrospun nanofibrous polymeric bandages: REVIEW ON WOUND DRESSINGS, Polym. Adv. Technol. 21 (2) (2010) 77–95, https://doi.org/10.1002/pat.1625.

[20] S. Huang, X. Fu, Naturally derived materials-based cell and drug delivery systems in skin regeneration, J. Control. Release 142 (2) (2010) 149–159, https://doi.org/10.1016/j.jconrel.2009.10.018.

[21] J. Necas, L. Bartosikova, P. Brauner, J. Kolar, Hyaluronic acid (hyaluronan): a reviewHyaluronic acid (hyaluronan): a review, Vet. Med. 53 (No. 8) (2008) 397–411, https://doi.org/10.17221/1930-VETMED.

[22] G. Kogan, L. Šoltés, R. Stern, P. Gemeiner, Hyaluronic acid: a natural biopolymer with a broad range of biomedical and industrial applications, Biotechnol. Lett. 29 (1) (2006) 17–25, https://doi.org/10.1007/s10529-006-9219-z.

[23] A. Shiedlin, R. Bigelow, W. Christopher, S. Arbabi, Evaluation of hyaluronan from different sources: Streptococcus zooepidemicus, rooster comb, bovine vitreous, and human umbilical cord, Biomacromolecules 5 (2004) 2122–2127, https://doi.org/10.1021/bm0498427.

[24] G. Benati, M.S. Bertone, Nutrition and wound healing, Meas. Wound Heal. Sci. Pract. 28 (2013) 63–71, https://doi.org/10.1007/978-1-4471-2987-5_4.

[25] J. Voigt, V.R. Driver, Hyaluronic acid derivatives and their healing effect on burns, epithelial surgical wounds, and chronic wounds: A systematic review and meta-analysis of randomized controlled trials: Hyaluronic acid and wound healing, Wound Repair Regen 20 (3) (2012) 317–331, https://doi.org/10.1111/j.1524-475X.2012.00777.x.

[26] K. Wang, R. Li, J.H. Ma, Y.K. Jian, J.N. Che, Extracting keratin from wool by using L-cysteine, Green Chem. 18 (2016) 476–481, https://doi.org/10.1039/C5GC01254F.

[27] M. Zoccola, A. Aluigi, C. Tonin, Characterisation of keratin biomass from butchery and wool industry wastes, J. Mol. Struct. 938 (1-3) (2009) 35–40, https://doi.org/10.1016/j.molstruc.2009.08.036.

[28] P. Wu, X. Dai, K.e. Chen, R. Li, Y. Xing, Fabrication of regenerated wool keratin/polycaprolactone nanofiber membranes for cell culture, Int. J. Biol. Macromol. 114 (2018) 1168–1173, https://doi.org/10.1016/j.ijbiomac.2018.03.157.

[29] K. Yamauchi, M. Maniwa, T. Mori, Cultivation of fibroblast cells on keratin-coated substrata, J. Biomater. Sci. Polym. Ed. 9 (3) (1998) 259–270, https://doi.org/10.1163/156856298X00640.

[30] A. Edwards, D. Jarvis, T. Hopkins, S. Pixley, N. Bhattarai, Poly(ε-caprolactone)/keratin-based composite nanofibers for biomedical applications: PCL/Keratin-Based Composite Nanofibers, J. Biomed. Mater. Res. 103 (1) (2015) 21–30, https://doi.org/10.1002/jbm.b.33172.

[31] P. Sierpinski, J. Garrett, J. Ma, P. Apel, The use of keratin biomaterials derived from human hair for the promotion of rapid regeneration of peripheral nerves, Biomaterials 29 (2008) 118–128, https://doi.org/10.1016/j.biomaterials.2007.08.023.

[32] C. Wang, S.N. Tong, Y.H. Tse, M. Wang, Conventional Electrospinning vs. Emulsion Electrospinning: A Comparative Study on the Development of Nanofibrous Drug/Biomolecule Delivery Vehicles, Adv. Mater. Res. 410 (2011) 118–121, https://doi.org/10.4028/www.scientific.net/AMR.410.118.

[33] P. McClellan, W.J. Landis, Recent Applications of Coaxial and Emulsion Electrospinning Methods in the Field of Tissue Engineering, Biores. Open Access 5 (2016) 212–227, https://doi.org/10.1089/biores.2016.0022.

[34] X. Li, Y. Su, S. Liu, L. Tan, X. Mo, S. Ramakrishna, Encapsulation of proteins in poly (l-lactide-co-caprolactone) fibers by emulsion electrospinning, Colloids Surf. B Biointerf. (2010), https://doi.org/10.1016/j.colsurfb.2009.09.014.

[35] L. Xiaoqianga, S. Yana, L. Shuipinga, Encapsulation of proteins in poly(L-lactide-co-caprolactone) fibers by emulsion electrospinning, Colloid Surf. B 75 (2010) 418–424, https://doi.org/10.1016/j.colsurfb.2009.09.014.

[36] Y. Zhao, X. Cao, L. Jiang, Bio-mimic multichannel microtubes by a facile method, J. Am. Chem. Soc. 129 (2007) 764–765, https://doi.org/10.1021/ja068165g.

[37] P. Kakkar, B. Madhan, G. Shanmugam, Extraction and characterization of keratin from bovine hoof: A potential material for biomedical applications, Springerplus. 3 (2014) 596, https://doi.org/10.1186/2193-1801-3-596.

[38] D.Y. Kang, W.S. Kim, I.S. Heo, Y.H. Park, S. Lee, Extraction of hyaluronic acid (HA) from rooster comb and characterization using flow field-flow fractionation (FlFFF) coupled with multiangle light scattering (MALS), J. Sep. Sci. 33 (2010) 3530–3536, https://doi.org/10.1002/jssc.201000478.

[39] B.C. Smith, Fundamentals of fourier transform infrared spectroscopy, second ed., CRC Press, 2011.

[40] S. Mohamadi, Preparation and Characterization of PVDF/PMMA/Graphene Polymer Blend Nanocomposites by Using ATR-FTIR Technique, in: Infrared Spectrosc. - Mater. Sci. Eng. Technol., 2012. doi:10.5772/36497.

[41] A. Chrambach, D. Rodbard, Polyacrylamide gel electrophoresis, Science 172 (1971) 440–451, https://doi.org/10.1126/science.172.3982.440.

[42] M. Skidmore, J. Turnbull, Separation and Sequencing of Heparin and Heparan Sulphate Saccharides. (2005) 179-201. doi:10.1016/B978-008044859-6/50007-1.

[43] U.K. Laemmli, Cleavage of structural proteins during the assembly of the head of bacteriophage T4, Nature (1970), https://doi.org/10.1038/227680a0.

[44] J. Yuan, J. Geng, Z. Xing, K. Shim, I. Han, J. Kim, Novel wound dressing based on nano fi brous PHBV – keratin mats, (2015) 1027–1035. doi:10.1002/term.

[45] K.J. Reddy, K.T. Karunakaran, Purification and characterization of hyaluronic acid produced by Streptococcus zooepidemicus, J. BioSci. Biotech. 2 (2013) 173–179.

[46] A.M. Vasi, M.I. Popa, M. Butnaru, G. Dodi, L. Verestiuc, Chemical functionalization of hyaluronic acid for drug delivery applications, Mater. Sci. Eng. C 38 (2014) 177–185, https://doi.org/10.1016/j.msec.2014.01.052.
[47] D.A. Grosenbaugh, D.M. Hood, Keratin and associated proteins of the equine hoof wall, Am. J. Vet. Res. (1992).
[48] S. Wang, F. Taraballi, L.P. Tan, K.W. Ng, Human keratin hydrogels support fibroblast attachment and proliferation in vitro, Cell Tissue Res. 347 (2012) 795–802, https://doi.org/10.1007/s00441-011-1295-2.
[49] Y. Zhang, K. Wu, H. Sun, J. Zhang, J. Yuan, Z. Zhong, Hyaluronic Acid-Shelled Disulfide-Cross-Linked Nanopolymersomes for Ultrahigh-Efficiency Reactive Encapsulation and CD44-Targeted Delivery of Mertansine Toxin, ACS Appl. Mater. Interf. (2018), https://doi.org/10.1021/acsami.7b17718.
[50] S. Kanchana, M. Arumugam, S. Giji, T. Balasubramanian, Isolation, characterization and antioxidant activity of hyaluronic acid from marine bivalve mollusc Amussium pleuronectus (Linnaeus, 1758), Bioact. Carbohydrates Diet. Fibre. (2013), https://doi.org/10.1016/j.bcdf.2013.06.001.
[51] D. Monticelli, V. Martina, R. Mocchi, R. Rauso, U. Zerbinati, G. Cipolla, N. Zerbinati, Chemical characterization of hydrogels crosslinked with polyethylene glycol for soft tissue augmentation, Open Access Maced. J. Med. Sci. (2019), https://doi.org/10.3889/oamjms.2019.279.
[52] A.N. Zelenetskii, S. Uspenskii, A. Zaboronok, G. Cherkaev, A. Shchegolihin, B. J. Mathis, M. Selyanin, T. Yamamoto, A. Matsumura, Polycomplexes of hyaluronic acid and borates in a solid state and solution: Synthesis, characterization and perspectives of application in boron neutron capture therapy, Polymers (Basel). (2018), https://doi.org/10.3390/polym10020181.
[53] V.H. Pomin, NMR chemical shifts in structural biology of glycosaminoglycans, Anal. Chem. 86 (2013) 65–94, https://doi.org/10.1021/ac401791h.
[54] L. Li, Y. Qian, C. Jiang, Y. Lv, W. Liu, L. Zhong, K. Cai, S. Li, L. Yang, The use of hyaluronan to regulate protein adsorption and cell infiltration in nanofibrous scaffolds, Biomaterials 33 (2012) 3428–3445, https://doi.org/10.1016/j.biomaterials.2012.01.038.
[55] Y. Wang, P. Li, P. Xiang, J. Lu, J. Yuan, J. Shen, Electrospun polyurethane/keratin/AgNP biocomposite mats for biocompatible and antibacterial wound dressings, J. Mater. Chem. B 4 (2016) 635–648, https://doi.org/10.1039/c5tb02358k.
[56] M. He, B. Zhang, Y. Dou, G. Yin, Y. Cui, X. Chen, M. Matsuo, D. Huang, H.-Y. Kim, Fabrication and characterization of electrospun feather keratin/poly(vinyl alcohol) composite nanofibers, RSC Adv. 7 (2017) 9854–9861, https://doi.org/10.1039/C6RA25009B.
[57] C.H. Chen, S.H. Chen, K.T. Shalumon, J.P. Chen, Dual functional core-sheath electrospun hyaluronic acid/polycaprolactone nanofibrous membranes embedded with silver nanoparticles for prevention of peritendinous adhesion, Acta Biomater. 26 (2015) 225–235, https://doi.org/10.1016/j.actbio.2015.07.041.
[58] M. Movahedi, A. Asefnejad, M. Rafienia, M.T. Khorasani, Potential of novel electrospun core-shell structured polyurethane/starch (hyaluronic acid) nanofibers for skin tissue engineering: In vitro and in vivo evaluation, Int. J. Biol. Macromol. 146 (2020) 627–637, https://doi.org/10.1016/j.ijbiomac.2019.11.233.
[59] S. Koombhongse, W. Liu, D.H. Reneker, Flat polymer ribbons and other shapes by electrospinning, J. Polym. Sci., Part B: Polym. Phys. 39 (2001) 2598–2606, https://doi.org/10.1002/polb.10015.
[60] H. Itoh, Y. Li, K.H.K. Chan, M. Kotaki, Morphology and mechanical properties of PVA nanofibers spun by free surface electrospinning, Polym. Bull. 73 (2016) 2761–2777, https://doi.org/10.1007/s00289-016-1620-8.
[61] T. Elzein, M. Nasser-Eddine, C. Delaite, S. Bistac, P. Dumas, FTIR study of polycaprolactone chain organization at interfaces, J. Colloid Interf. Sci. 273 (2004) 381–387, https://doi.org/10.1016/j.jcis.2004.02.001.
[62] R.P. Gonçalves, F.F.F. da Silva, P.H.S. Picciani, M.L. Dias, Morphology and Thermal Properties of Core-Shell PVA/PLA Ultrafine Fibers Produced by Coaxial Electrospinning, Mater. Sci. Appl. 06 (2015) 189–199, https://doi.org/10.4236/msa.2015.62022.
[63] A.O. Basar, S. Castro, S. Torres-Giner, J.M. Lagaron, H. Turkoglu Sasmazel, Novel poly(ε-caprolactone)/gelatin wound dressings prepared by emulsion electrospinning with controlled release capacity of Ketoprofen anti-inflammatory drug, Mater. Sci. Eng. C. 81 (2017) 459–468. doi:10.1016/j.msec.2017.08.025.
[64] J. Nie, Z.L. Wang, J.F. Li, Y. Gong, J.X. Sun, S.G. Yang, Interface hydrogen-bonded core-shell nanofibers by coaxial electrospinning. Chinese, J. Polym. Sci. 35 (8) (2017) 1001–1100, https://doi.org/10.1007/s10118-017-1984-8.
[65] P. Taepaiboon, U. Rungsardthong, P. Supaphol, Drug-loaded electrospun mats of poly(vinyl alcohol) fibres and their release characteristics of four model drugs, Nanotechnology. 17 (2006) 2317–2329, https://doi.org/10.1088/0957-4484/17/9/041.
[66] S. Koocheki, S.S. Madaeni, P. Niroomandi, Development of an enhanced formulation for delivering sustained release of buprenorphine hydrochloride, Saudi Pharm. J. 19 (2011) 255–262, https://doi.org/10.1016/j.jsps.2011.05.001.
[67] R.L. Fischer, M.G. McCoy, S.A. Grant, Electrospinning collagen and hyaluronic acid nanofiber meshes, J. Mater. Sci. - Mater. Med. 23 (2012) 1645–1654, https://doi.org/10.1007/s10856-012-4641-3.
[68] S. Surucu, H. Turkoglu Sasmazel, Development of core-shell coaxially electrospun composite PCL/chitosan scaffolds, Int. J. Biol. Macromol. 92 (2016) 321–328, https://doi.org/10.1016/j.ijbiomac.2016.07.013.
[69] M. Yagi, N. Sato, Y. Mitsui, M. Gotoh, T. Hamada, K. Nagata, Hyaluronan Modulates Proliferation and Migration of Rabbit Fibroblasts Derived From Flexor Tendon Epitenon and Endotenon, J. Hand Surg. Am. 35 (2010) 791–796, https://doi.org/10.1016/j.jhsa.2010.02.010.
[70] C. Wang, J. Wang, L. Zeng, Z. Qiao, X. Liu, H. Liu, J. Zhang, J. Ding, Fabrication of electrospun polymer nanofibers with diverse morphologies, Molecules 24 (2019), https://doi.org/10.3390/molecules24050834.